REPORT DOCUMENTATION PAGE

AFRL-SR-BL-TR-98-
0553

1. AGENCY USE ONLY *(Leave blank)*	2. REPORT DATE	3. REPORT TYPE AND DATES COVERED
	5 June 1998	Final Technical Report 1 Feb 95 to 31 Jan 98

4. TITLE AND SUBTITLE
Microstructural and Mechanistic Study of Primary Creep in titanium alloys at Lower Temperatures

5. FUNDING NUMBERS
F49620-95-1-0153

6. AUTHOR(S)
Professor Michael J. Mills

7. PERFORMING ORGANIZATION NAME(S) AND ADDRESS(ES)
Department of Materials Science and Engineering
The Ohio State University
477 Watts Hall
Columbus, OH 43210-1179

8. PERFORMING ORGANIZATION REPORT NUMBER

9. SPONSORING/MONITORING AGENCY NAME(S) AND ADDRESS(ES)
AFOSR/NA
110 Duncan Avenue, Ste B115
Bolling AFB, DC 20332-8050

10. SPONSORING/MONITORING AGENCY REPORT NUMBER
F49620-95-1-0153

11. SUPPLEMENTARY NOTES

19980803 100

12a. DISTRIBUTION AVAILABILITY STATEMENT
Approved for public release; distribution unlimited.

12b. DISTRIBUTION CODE

13. ABSTRACT *(Maximum 200 words)*

Primary creep is a dominant mode of deformation for commercial, two-phase alpha-beta titanium alloys such as Ti-6242 which are used extensively in the fan and compressor sections of jet aircraft engines. This program has improved our understanding of the mechanisms and phenomenology of primary creep in these alloys. Using a phenomenological approach based on the Holomon equation, we have shown that the extensive low temperature creep behavior is linked to the exceptionally small values of strain hardening exponent exhibited by these alloys, and that the long term creep response can be predicted from the results of short-term, constant-strain rate tests. This insight has suggested possible processing paths for improving the creep response of these materials, including the minimization of short-range ordering. A second focus of the program has shown that the Widmanstatten colony structure exhibits a dramatic plastic anisotropy. Single colony crystals of Ti-5Al-2.5Sn-0.5Fe, were obtained in collaboration with J. M. Scott of UES and Wright Laboratory. Extensive TEM investigation has revealed that this anisotropy can be directly correlated with the transmission of dislocations across the beta laths, and the accumulation of residual dislocation content near the interfaces. This information is essential in order to better model creep deformation in these materials.

14. SUBJECT TERMS

15. NUMBER OF PAGES
26

16. PRICE CODE

17. SECURITY CLASSIFICATION OF REPORT	18. SECURITY CLASSIFICATION OF THIS PAGE	19. SECURITY CLASSIFICATION OF ABSTRACT	20. LIMITATION OF ABSTRACT
Unclassfied	Unclassified	Unclassified	UL

Microstructural and Mechanistic Study of Primary Creep in Titanium Alloys at Lower Temperatures

A Final Report for

AFOSR Grant Number F49620 - 95 - 1 - 0153

Submitted to:

AFOSR/PKA
110 Duncan Avenue, Suite B115
Bolling Air Force Base, D.C. 20332-8050
Attention: Karen Buck

Submitted by:

Principal Investigator: Professor Michael J. Mills

Department of Materials Science and Engineering
The Ohio State University
477 Watts Hall
Columbus, OH 43210-1179

5 June 1998

OBJECTIVES

Primary creep is the dominant mode of deformation for titanium alloys at lower temperatures under most service conditions. Significant levels of creep strain may occur at stresses which are well below the yield strength of these alloys. The goals of this research program have been to ascertain the mechanisms which contribute to primary creep at lower temperatures and to determine the influence of the prominent microstructural elements on primary creep in these alloys.

APPROACH

Key characteristics of deformation include (a) very planar slip, (b) slip transmission across α/β boundaries, and (c) sliding at α/β, colony and grain boundaries. While these characteristics have been identified under various conditions previously, the mechanisms by which they occur and their influence on the primary creep behavior are not well understood. In this program, monotonic creep, stress change/ strain transient experiments, and constant strain rate tests are being performed on two classes of alloys. Binary, single phase α alloys (Ti-2Al and Ti-6Al) are being tested to study solute and short-range order (SRO) effects. Two-phase, near-α and α/β alloys (Ti-5Al-2.5Sn-0.5Fe and Ti-6Al-2V-4Sn-2Zr, respectively) are being tested to determine the effects of phase and colony boundaries on creep behavior. Oriented crystals of both single and two-phase materials are being produced with the support of Wright Laboratories. These crystals are enabling us to examine the creep response of individual slip systems, as well as to isolate the effects of key microstructural elements in the two-phase alloys. Characterization of localized slip and interface sliding is being conducted with the aid of fine fiducial grids using SEM. Dislocation microstructures and dislocation/interface interactions are being studied extensively for the first time in these alloys using TEM. Polycrystalline samples of these alloys are also being tested in order to determine aggregate behavior. A new annealing treatment which potentially holds promise for improving the creep strength, work hardening characteristics and fatigue properties of titanium alloys containing significant volume fractions of α phase has also been identified.

SUMMARY OF PROGRAM

Progress has been made in demonstrating the usefulness of a simple, phenomenological model of transient flow which has been devloped during this program for primary creep displaying power-law behavior in time. Based on Hollomon parameters obtained from constant strain rate testing, a fairly accurate prediction of the long-time primary creep response has been demonstrated for both single phase and two phase alloys. Testing of single colony crystals of Ti-5Al-2.5Sn-0.5Fe has continued for several orientations and stress levels. These tests have revealed that individual colonies exhibit significant plastic anisotropy, an effect most prominent under creep conditions. Detailed TEM study of the

dislocation processes associated with the slip transmission process between the α and the β phase has been been completed for two orientations showing the largest disparity in creep strength. We believe that we can reconcile the hardening characteristics of these crystals based on these observations. TEM investigation of creep deformed, single phase Ti-6Al alloys has also been performed for the first time. The remarkably planar mode of deformation characteristic of constant strain rate deformation of these alloys is also observed under creep conditions. Optical microscopy of interrupted tests has revealed the overall evolution of deformation in these polycrystals, and have helped shape our present approaches to modeling this transient behavior. During the past year we have published our results in one journal article and two conference proceedings, and have collectively (graduate students and PI) made 6 conference presentations on our work.

Attempts to grow single-phase single crystals of Ti-2 wt%Al and Ti-6 wt%Al in collaboration with Mike Scott at Wright Laboratories have been unsuccessful, due primarily to a moderate Fe content (approximately 800 wt ppm) which makes the growth of single phase material impossible. A new batch of Ti-6Al alloy has been requested of Duriron Inc. of Dayton, who originally suppied the binary alloys. In addition, high purity buttons of Ti-6Al are presently being prepared by RMI Titanium of Niles, OH which will provide us with an additional supply of high quality material for single crystal and polycrystal testing.

The confluence of our phenomenological and microstructural understanding of primary creep in these alloys has also yielded an exciting new path of investigation. These alloys typically exhibit moderate strain rate sensitivity and quite low strain hardening exponents. Based on our phenomenological description of primary creep, large, time-dependent creep strain are anticipated. On the premise that the low strain hardening exponents are fundamentally due to the highly planar nature of slip in the α-phase, which arises due to short-range ordering (SRO), we have recently begun to explore simple thermal treatments to minimize or eliminate short range ordering. Short-range order minimization has been explored first in single-phase Ti-6Al, and dramatic improvements to the strain hardening characterisitics of this material have been demonstrated. While we intend to broaden our investigation of SRO minimization to commercial two-phase alloys such as Ti-6Al-4V and Ti-6242. The initial encouraging results on the single phase material has prompted us to file an invention disclosure for SRO minimization, which has the potential of improving the creep strength and work hardening charateristics of a wide range of titanium alloys, and could have wide-ranging benefits for both producers and consumers of titanium alloys. We intend to proceed with the patent process assuming the same beneficial efects are obtained with the commercial titanium alloys.

1. Phenomenological Treatment of Primary Creep

While it has long been recognized that Ti alloys exhibit extensive primary creep behavior at lower temperatures [1-6], the specific materials characteristics responsible for this behavior had not been previously identified. In several previous investigations of primary creep in Ti alloys at ambient temperatures, creep transients have been found to fit a power law expression of the form

$$\varepsilon = A\, t^{a} \qquad [1]$$

with a value for a of the order of 0.2-0.3. This form has been reported for both single phase and two-phase α–β microstructures, and indicates that although the creep rate decreases continually with time, true saturation is not achieved.

We have employed a well-established phenomenological description for plastic flow under constant strain rate conditions, namely the Hollomon-type constitutive expression:

$$\sigma = K\, \varepsilon^{n}\, \dot{\varepsilon}^{m} \qquad [2]$$

We have found that this expresssion provides a reasonable description of the flow curves for both single phase Ti-6wt%Al and Ti-6242 in several microstructural conditions. The values of n, m, and K for several cases are listed in Table I. Paralleling a development by Lubahn [7], it can also be shown that if the Hollomon equation is obeyed, then the power law expression of Equation 1 for the creep transient is expected, and the parameters A and a can then be expressed in terms of the Hollomon parameters as:

$$a = \frac{m}{m+n} \qquad [3]$$

$$A = \left(\frac{\sigma}{K}\right)^{\left(1/m+n\right)} \cdot \left(\frac{m+n}{m}\right)^{\left(m/m+n\right)} \qquad [4]$$

This phenomenological description would appear to have merit, particularly at longer creep times based on the work to be presented below on both two-phase Ti-6242 and single-phase Ti6Al.

1.1 Results for Ti-6242

In order to determine whether this approach is valid for Ti alloys, constant strain rate and creep tests are being conducted to examine the correlation between deformation modes in a Ti-6Al-2V-4Sn-2 Zr (Ti-6242) colony microstructure, shown in Fig. 1. Constant strain rate testing is used to generate values of n, m and K. These strain measurements were performed using strain gages mounted directly on the

Table I Comparison of yield strengths and constants from constant strain rate and creep tests for single phase (two heat treatments) and two phase Ti alloys. Results for commercial processing and a novel heat treatment designed to minimize SRO in the single phase alloy

Material	σ_y	n	m	K	A	a
Convetional Processing						
Ti-6%Al (α anneal/slow cooled)	772 MPa	0.03	0.011	965 MPa	0.0008	0.25
Ti-6242 (lath)	978 MPa	0.063	0.015	1546 MPa	0.00023	0.19
Novel Heat Treatment						
Ti-6%Al (α anneal/water quench)	772 MPa	0.14	——	1585 MPa	0.006	0.07

compression sample in order to obtain accurate measurement of the microstrain regime. Creep tests at two different stress levels - 80% and 95% of the yield strength - was performed. Care was taken to accurately measure the small time strains. This was done to determine if the long time exponent of 0.2 that has been widely been reported in the literature also held at small times. Fig. 2 a shows the stress strain plot for two different strain rates and Fig. 2 b shows the corresponding true stress vs true strain plot on a log-log scale. It can be seen that the Holloman equation provides a reasonably good fit to the data at smaller strains. The resulting values of yield strength, n, m and K are also provided in Table II. The predicted values of a for creep conditions are also indicated which are calculated using Eqn. (1). Creep tests at the two different stress levels are shown in Fig. 3 a. It is interesting to note that although the longer time exponent is 0.2, creep curves at smaller times for both the stress levels show a large time exponent of 0.8. Fig. 3 b compares the calculated creep curves obtained using the Hollomon parameters in Table I with the experimental data. A reasonable agreement between the calculated and experimental values were obtained.

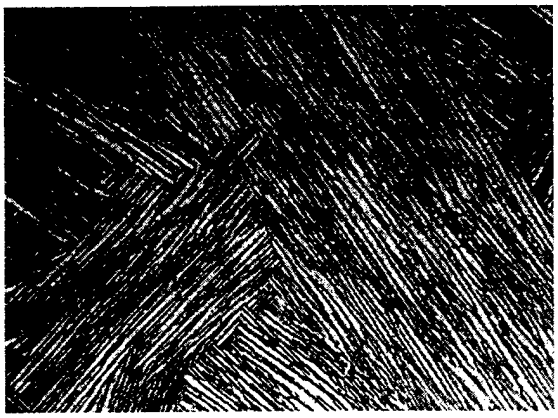

Fig. 1 Colony microstructure for two phase Ti-6242 alloy.

Creep tests were also performed on a Widmanstatten basketweave microstructure at two different stress levels of 80 and 90% of its yield strength. It is interesting to note, Fig. 4 that the creep curves again show two disticnt regimes, an initial larger exponent which decays to 0.2 at longer times. It is clear from data in the literature and from the present measurements that the long time **a** values are independent of stress levels and microstructure.

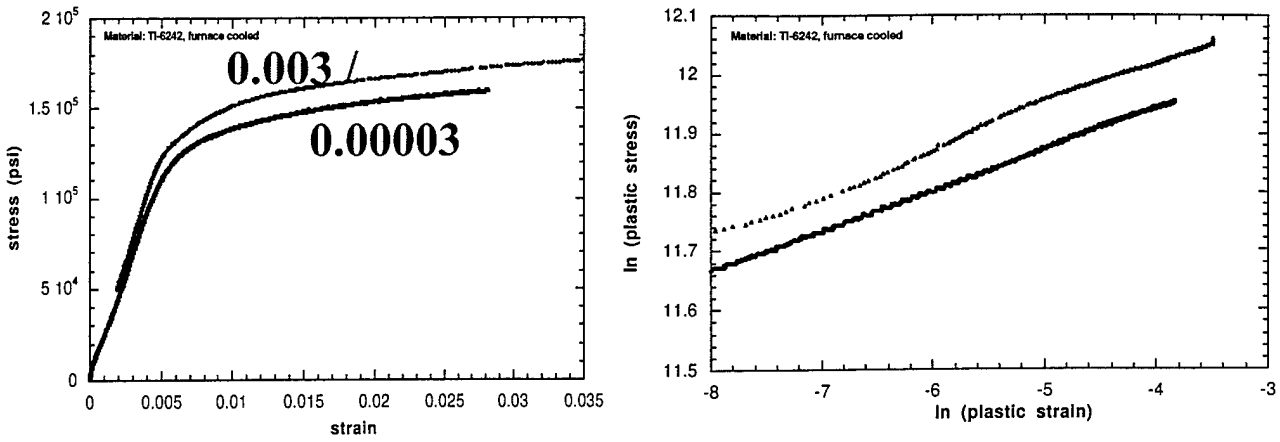

Fig. 2 Stress - strain plot for Ti-6242 in the colony microstructure (a) linear-linear, (b) log-log plot.

Fig. 5 compares the creep curves for two different microstructures for Ti-6242 at the same stress level. Consistent with observations in the literature, the basketweave microstructure was found to be more creep resistant. The literature attributes this resistance to the smaller colony size and consequently smaller slip lengths in the basketweave microstructure. However, the results obtained using the oriented single colony crystals, which are discussed in the following section suggest that a simple slip length argument based on the Burgers orientation relationship between the two phases does not completely describe the issues related to differences in creep resistance.

Table II n, m, K, and a values for Ti-6242

n	**0.063**
m	**0.015**
K	**22.45 X 10^4**
a	**0.191**

1.2 Results for Ti-6Al

Creep tests were performed at stress levels of 93.4% and 79% of the yield strength on a single phase Ti-6Al alloy. Careful analysis of the loading transient indicates that the strain, while the sample is being loaded, is elastic in nature. Once the load is completely applied, all measured strain is due to creep deformation. The log-log plot of this creep data is shown in Fig. 6. Three regimes designated as I, II and III,with different time exponents was observed. The initial time exponent in Regime I is about 0.2 for both data sets. Regime II has a larger time exponent approaching 0.4, implying slower exhaustion. Regime III (the long time regime) once again shows a decline in the time exponent to about 0.2. The time exponent in Regime III is comparable to the value obtained by Odegard and Thompson [3] for Ti-

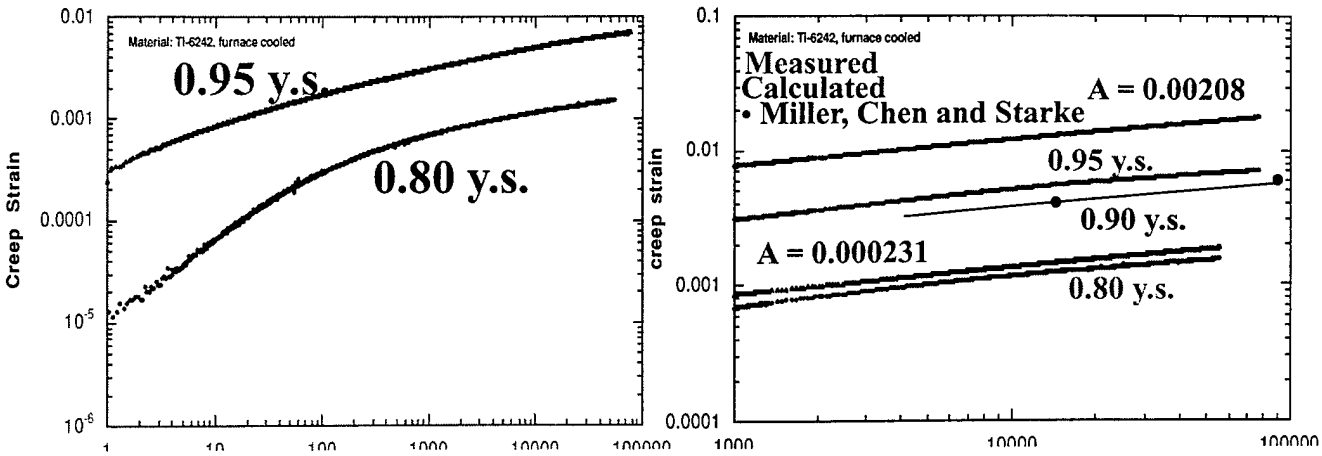

Fig. 3 a Experimental creep curves at two different stress levels for colony microstructure, (b) Comparison of experimental and calculated creep curves. Calculated creep curves obtained by using Hollomon parameters from Table I.

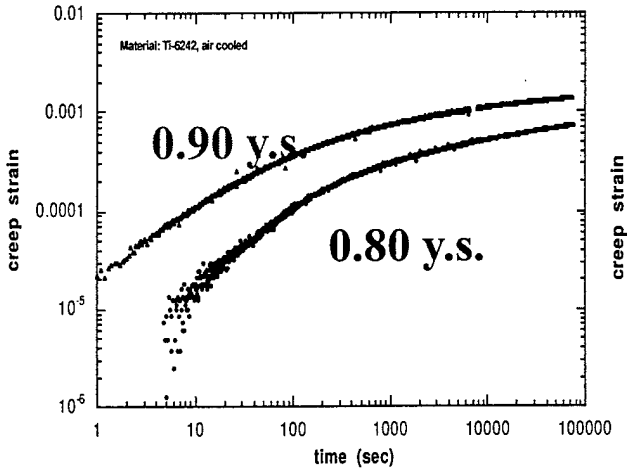

Fig. 4 Creep curves for Widmanstatten basketweave microstructure for Ti-6242.

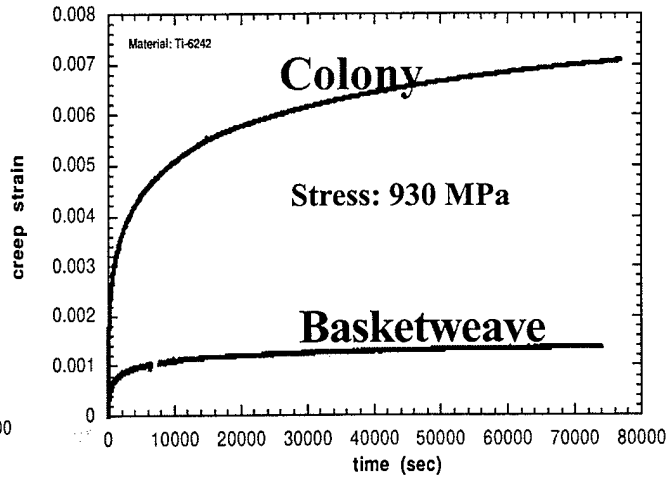

Fig. 5 Comparison of creep curves for two different microstructures at the same stress levels.

5Al -2.5Sn.

An interrupted creep test was performed at a stress level of 93.4% of the yield strength of Ti-6Al to study the evolution of surface slip lines in the three Regimes as a function of time. Optical micrographs, Fig. 7 indicate that in Regime I, slip is very inhomogeneous and the deformation is concentrated in coarse slip bands. As discussed below, dislocations tend to be arranged in a highly planar

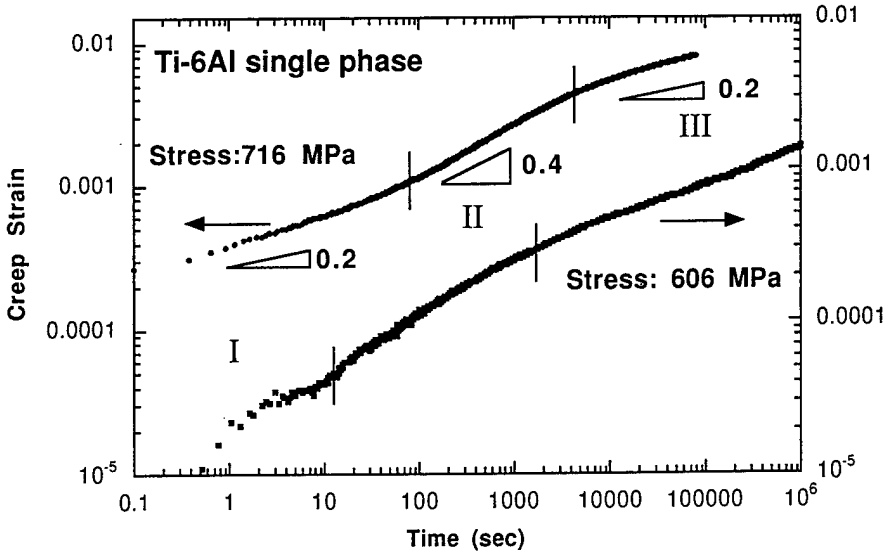

Fig. 6 Log-log plot of creep strain vs creep time for Ti-6Al tested at two different fractions 93.4%(716 MPa) and 79% (606 MPa) of the yield strength.

arrays following deformation. Slip lines, with an interline spacing of tens of microns, are observed only in a few grains. These slip lines appear to extend all the way across the active grains after a short time (≈10s). In Regimes II and III, it was observed that new slip lines initiate in grains neighboring those active in Regime I. These slip lines were observed to originate from the grain boundaries and grow very slowly with time, in contrast to the slip lines formed in Regime I. In addition, new slip lines were formed as a function of time leading to finer and finer spacing between the lines. Intensification of the existing slip lines (including those that were formed in Regime I) was observed throughout the test.

A possible explanation for these observations is that slip is first initiated in the more favorably-oriented grains in Regime I. The applied stress level could be much higher than the critical resolved shear stress (CRSS) for these "easy slip" grains, leading to rapid propagation of slip bands to the grain boundaries. Rapid exhaustion ensues due to the interaction of the dislocation arrays in the bands with grain boundaries. In Regime II, new slip bands are initiated in the adjoining grains due to either compatibility requirements or slip transmission. This would be consistent with the experimental observation that the slip lines are nucleated near the grain boundaries in Regime II and III. Since the new bands in Regime II propagate into undeformed grains at a much slower rate than the propagation in Regime I, the rate of exhaustion in this regime is lower (i.e. the value of α is larger). In Regime III, the interaction between slip bands could once again cause exhaustion of the creep rate. It was also observed that a large number of the "new slip bands" have reached grain boundaries in Regime III. Slip lines formed during Regimes II and III are observed to grow with time, which is consistent with a compatibility requirement

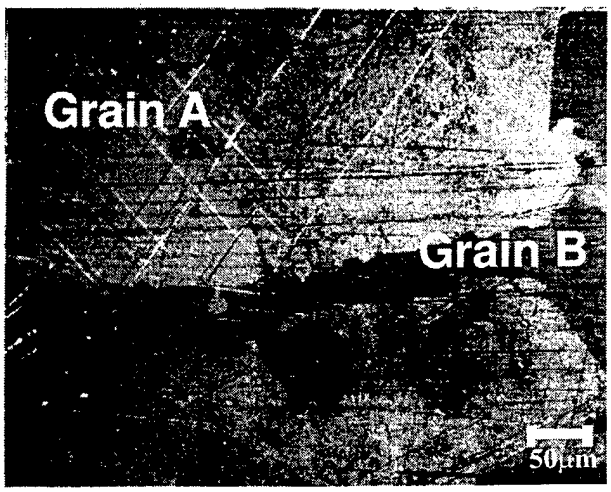

Fig. 7 (a) Shows the presence of coarse slip in grain A in regime I.

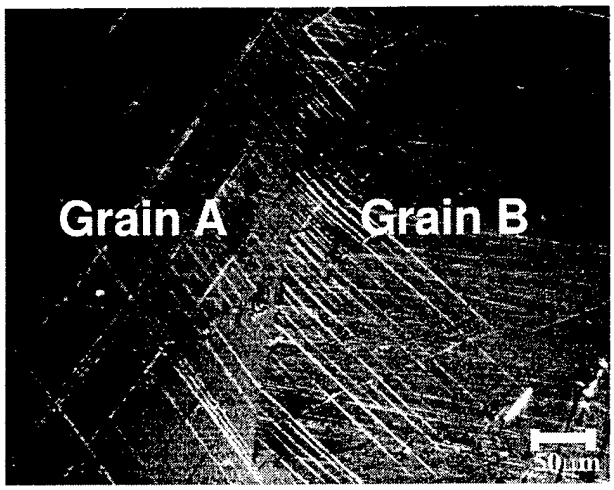

Fig. 7 (b) Shows the nucleation of slip lines at the grain boundary into grain B due compatibility requirements. Picture taken in regime II.

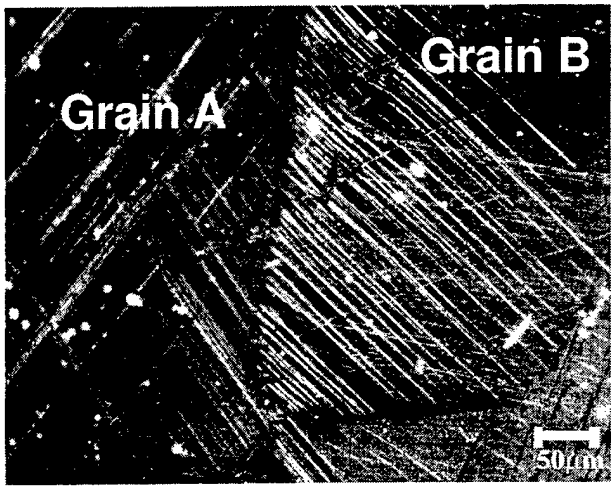

Fig. 7 (c) Shows the intensification of existing slip line and nucleation new slip lines in both grains A and B. Picture taken at the start of regime III.

picture. As these new slip bands are being formed in grains that do not seem to be favorably oriented for slip, their formation can be attributed primarily to high local stresses at the grain boundaries. Hence, as the slip band propagates into the grain, the stress imposed on the leading dislocations in the band should decrease continuously with time, leading to ever slower propagation of the band . These bands generally do not stop propagating into the grain in the time period of these tests. This implies the continual presence of high local stresses at grain boundaries. The "original slip bands" formed in the "easy slip" grains in Regime I continue to intensify with time and provide the stress concentration needed at the grain boundaries. The intensification of the "original slip bands" also causes nucleation

of new slip bands at the grain boundaries with time.

Relating the observations of the single phase alloy (Fig. 6) to the creep data for the two-phase alloys described earlier, we note that Regime I does not appear to be present. This may be due to the relative scale of the microstructures. The average grain size for the single phase alloy is about ≈500μm, which is an order of magnitude larger than individual α lath spacings for the two-phase Ti-6242. Thus, the initial rapid propagation of favorably oriented slip bands may occur too rapidly and produce too little strain to be measurable macroscopically.

1.3 Observation of Negative Creep in Single Phase Ti-6Al

During the interrupted creep test the sample was loaded and unloaded four times to study the evolution of surface slip lines. Negative creep was observed during the third and fourth loading of the sample. Fig. 8 shows the occurence of negative creep during the fourth loading. The negative creep strains were measured to be εneg= 0.00044 (third loading) and εneg = 0.00013 (fourth loading). These strains are small and they were accumulated over a short period of time, approximately 30-50 sec as shown in figure . It should be noted that negative creep is unlike a yield point behavior in a constant strain rate test because in this case the sample actually expands under stress (for compression). While this is a very unsusual result, similar behavior has been observed before in Ti alloy systems. Thompson and Odegard [2] observed negative creep in their work on low temperature creep of Ti-6Al-4V. They were studying the effect of pre-strain on the primary creep behavior. Significant negative creep was observed on those samples which experienced the largest pre-strain and were subsequently tested at a stress level of 70% of the yield strength. Their data is shown in Fig. 9. One important similarity between the two results is that negative creep was observed only after significant pre-strains. There are several important differences between our results and that of Thompson and Odegard's. a) Negative creep was observed at a stress level of 93.4% ys in our case where as it was observed at 70% of ys in their case. b)Negative creep strains acccumulated over the order of hours in Thompson and Odegard's experiment , where as it was accumulated over 10s of seconds in our case. It should be noted that the first data point was taken at 0.1 hours by Thompson and Odegard in their creep tests. Hence, it is possible that negative flow was present in their 80%ys and 90%ys data, but that it dissipated prior to their first measurement. The observation of negative creep after loading is very remarkable because no back flow was observed in our tests even after complete removal of the load, although the microstructure consists predominantly of planar arrays of dislocations. Thompson and Odegard did not offer an explanation for their results. We intend to pursue the characterization of this remarkable behavior by conducting controlled stress decrement and increment experiments. While the strains associated with this effect are small, such unexpected shape changes may be importnat to consider for small-tolerance applications. Further study of the negative creep flow may also yield additional information concerning the unique dynamics associated with the dislocation arrays in the α-phase.

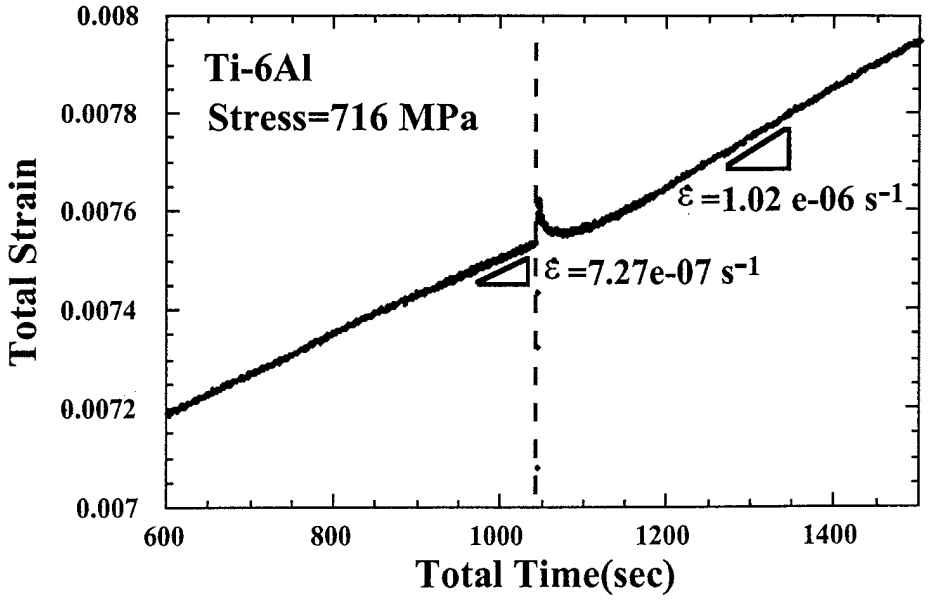

Fig. 8 Plot of creep strain vs creep time of Ti-6Al showing the occurence of negative creep.

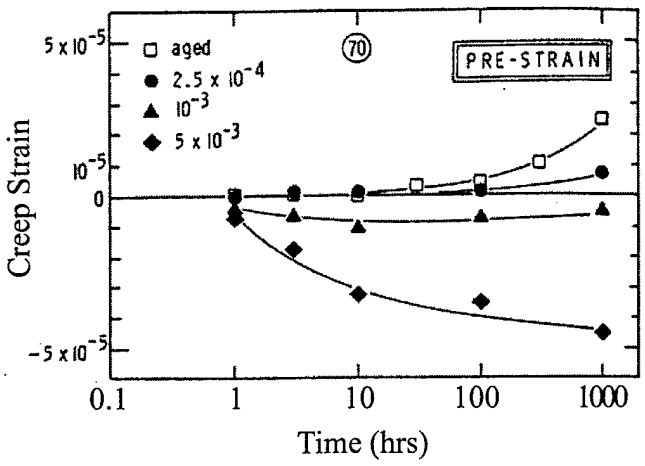

Fig. 9 Thompson and Odegard data on low temperaure creep of Ti-6Al-4V showing negative creep in pre-strained samples.

A final indication that this phenomenological description has merit, particularly at longer creep times, is shown in Fig. 10 in which creep data for Ti-6Al and Ti-6242 with a colony lath structure are compared with corresponding creep curves which were predicted using the Hollomon parameters (and Equations 3 and 4).

The deviations between observed and predicted curves in all the cases described above are believed to be due to the inability of the Hollomon law to fit the constant strain rate data in the small strain regime, and the fact that the experiments were conducted under constant stroke instead of constant sample displacement. Efforts are underway to control the stroke of the machine using a Linear Variable Displacement Transducer (LVDT) attached right on the platen of the compression cage. This is expected to give better strain rate control in the small strain region and hence, more precise measurement of Hollomon parameters in the small strain regime. Improvements in the fitting procedure are also presently underway.

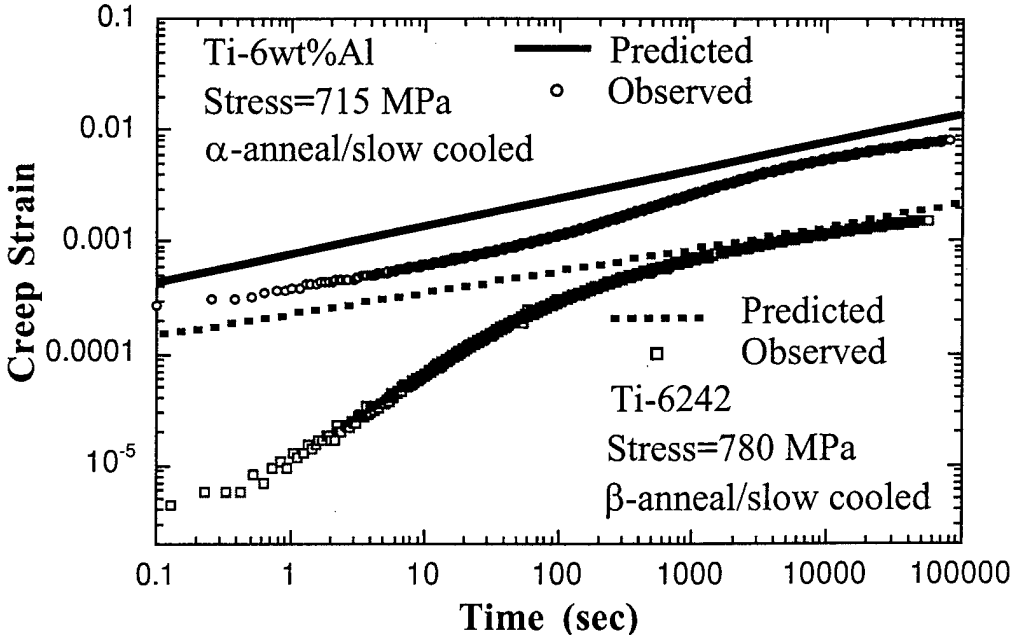

Fig. 10 Comparison of experimental and predicted creep response for single and two phase Ti alloys at room temperature. Note convergence of predicted and experimental data at longer times.

2. Oriented Single Colony Crystals

2.1 General Orientation Considerations

A Burgers OR between the α (hcp) and the β (bcc) phases has widely been reported in the literature for Ti alloys [8,9].

$$(101)_\beta \parallel (0001)_\alpha, [1\bar{1}\bar{1}]_\beta \parallel [2\bar{1}\bar{1}0]_\alpha \qquad (5)$$

A consequence of the Burgers OR is that the prismatic glide plane in α is parallel to the $\{112\}_\beta$ glide plane in the β phase. A detailed analysis of the alloy used in this study shows that the Burgers OR is not exactly followed. The closest packed planes in the α and the β phase were misaligned by 0.78°. The Burgers vector $\mathbf{a_1}$ in the α phase is nearly parallel to the Burgers vector $\mathbf{b_1}$ in the β phase (off by 0.56°), Fig. 11. However, it is clear from Fig. 11 that there is a significant 10° misalignment between the slip vectors $\mathbf{a_2}$ and $\mathbf{b_2}$ in the α and β phase respectively. No corresponding slip vector exists in the β phase for the slip vector $\mathbf{a_3}$ in the α phase.

As a consequence of these misallignments, it is expected that the creep properties of single colony crystals oriented

for $\mathbf{a_1}$ prismatic (OA) vs $\mathbf{a_2}$ prismatic (OB) slip will be anisotropic. This result was clearly demostrated in the previous report, with the OB colony crystal much more creep resistant than the OA crystal. TEM analysis of the microstructures was made to study the interaction of the dislocations with the broad and side face of the interfaces.

2.2 TEM Observations for Orientation B

2.2.1 Interaction with Broad Face in Orientation B

The WB TEM micrograph in Fig. 12 shows the sheared β region from the front face for colony orientation B, tested at 80% y.s. followed by a stress increase to 95%.y.s. In this view, the **a2** dislocations and especially the edge segments interact with the broad face of the β lath. It was difficult to see the edge interaction, even with the large tilt used, since the foil was cut steep angle to the glide plane. The **a2** screws are seen shea lath are $\mathbf{b_2}=1/2[\bar{1}11]$.

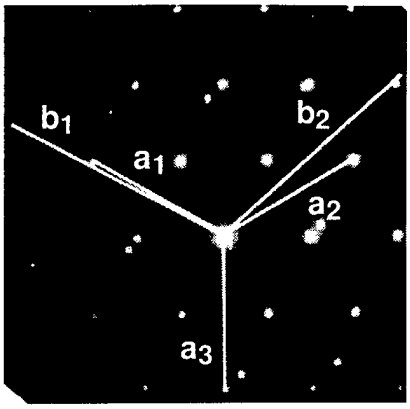

Fig. 11 Diffraction pattern along $(101)_\beta \parallel (0001)_\alpha$ showing the allignment of the slip vectors in the two phases.

The WB TEM micrograph in Fig. 13 shows the same sheared β region wherein both the **a2** and **b2** dislocations are out of contrast. However, the interface region where the shearing has occurred, showed a strong residual dislocation contrast similar to contrast that was seen in the side face interaction. Presently, the character of these dislocations has not been determined. In the breakthrough regions, **a1** activity was observed.

2.2.2 Interaction with Side Face in Orientation B

Fig. 14 shows the side face interaction of $\mathbf{a_2}=[\bar{1}2\bar{1}0]$ screw dislocation pile up with the β lath for colony orientation B, tested at 90% yield strength. Arrays of $\mathbf{a_2}=[\bar{1}2\bar{1}0]$ dislocations are seen on either side of the β lath. The slip seems to be progressing in the direction of the arrow since the length of the pile up on exit side of the lath is shorter than the entry side. The slip transmission from α to β lath has occured though the β slip is not seen here. In this diffraction condition with $g=[\bar{1}10\bar{1}]_\alpha$, the dislocations $\mathbf{a_1}=[2\bar{1}\bar{1}0]$ dislocations should also be visible, but they are not present. However, some residual contrast from $\mathbf{a_3}=[\bar{1}\bar{1}20]$ disocations that are invisible with this **g** can be seen near the sheared region.

Fig. 15 shows the same sheared region with a different diffraction condition wherein the **a2**-pile up in the α phase as well the sheared region in the β lath are seen. The sheared region of the β lath mostly contain $\mathbf{b_2}=1/2[\bar{1}11]$ dislocations and the trace analysis has shown them as mostly edge in character

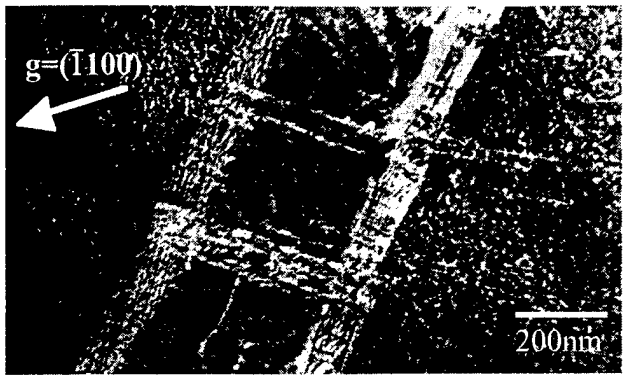

Fig. 12 WB micrograph showing the front face interaction for colony orientation B, tested at 80% y.s. followed by a stress increase to 95% y.s.

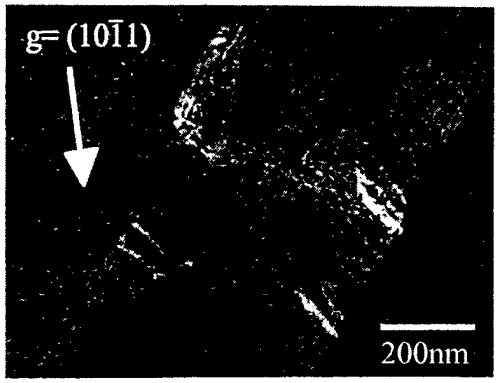

Fig. 13 WB micrograph showing the residual dislocation (b_r) contrast from the sheared region of the α/β interface

and lie on (12$\bar{1}$) plane. In this diffraction condition with $g=[1\bar{1}00]_\alpha$, **a3**=[$\bar{1}\bar{1}$20] disocations that are present near the sheared region (refer to Fig. 15) are however invisible.

In Fig. 16, all of the **a2**-dislocations in the pile up are out of contrast and the dislocations that are seen in the micrograph are **a3**=[$\bar{1}\bar{1}$20] dislocations. These **a3**- dislocations are seen on either side of the β lath, where the slip transfer has occurred, suggesting that they could be the by-product of the shearing process.

TEM micrograph (Fig. 17) shows another slip transfer region from the side face interaction of **a2**=[$\bar{1}$2$\bar{1}$0] screw dislocations with the β lath. Here, the slip seems to be progressing in opposite directions in the

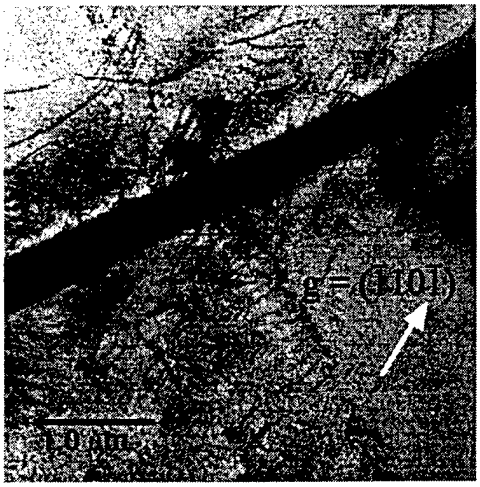

Fig.14 TEM micrograph showing the side face interaction.

Fig. 15 Magnified view of the sheared β lath from fig.

neighboring regions. This conclusion was arrived by examining the bowed out dislocations inside the beta lath at the sheared regions. The pile up in the alpha region again are of **a2** character and the β lath contain **b2**=1/2[$\bar{1}$11] dislocations. Both the edge and the screw segments of b_2 dislocations loops can be seen inside the β lath and they lie on (12$\bar{1}$) plane. The a_3- disocations that are present near the sheared region (refer to Fig. 15) are however out of contrast here.

The WB TEM micrograph (Fig. 18) shows same region the sheared β region wherein one can observe the **b2** loops originating at the interface from the **a2**-pile up (though not seen here) and expand on their glide plane as slip transfer progresses with time. With the emergence of successive loops, the previous ones are displaced in the interface, away from the source (in our case the shearing region). It is worthwhile to point out that they are still attached to the interface and seem mobile.

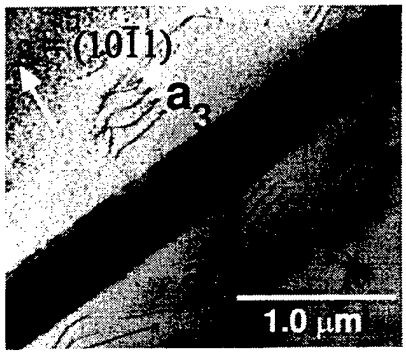

Fig. 16 $\mathbf{a_3}$ dislocations moving away from the interface on either side.

Fig. 19 shows the another sheared region wherein the entire glide plane in the β lath can be seen. The arrows indicated here shows the contrast from residual dislocations (**br**) that are created at the interface due to slip transmission. Their character has not been determined yet. However, the dislocations that are seen inside the β lath are presumably **b1**=1/2[11$\bar{1}$], since the **b2**=1/2[$\bar{1}$11] dislocations are out of contrast with this **g**. The origin of these **b1**s are presently unknown.

2.3 Modelling of β Shearing Process

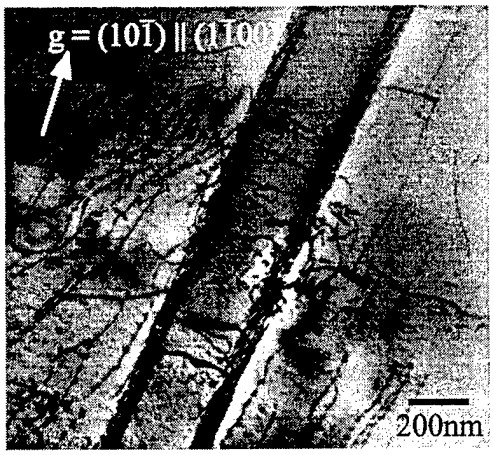

Fig. 17 BF Micrograph showing another sheared region of the side face interaction of OR B sample

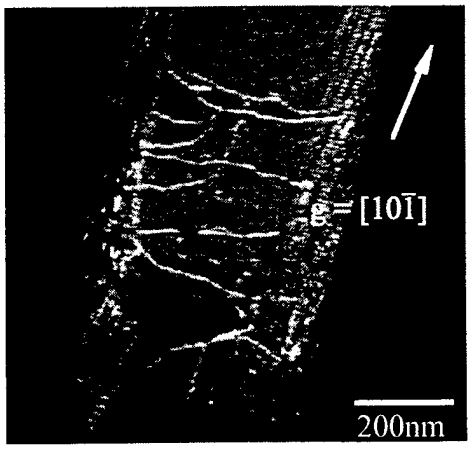

Fig. 18 WB micrograph showing the propagation of $\mathbf{b_2}$ loops inside β lath

In OA crystals, the edge component (using a foil with its normal parallel to $[0001]_\alpha$) of the dislocation loops shear through the broad face of the α/β interface and a one-to-one correpondence between the dislocations on either side of the β lath was observed, as discussed in more detail in last year's report. For OA crystal, the allignment of slip system in the two phases suggests that the slip transfer mechanism involves a simple dislocation transfer mechanism. However, it is interesting to note that

$$\frac{|b_\alpha|}{|b_\beta|} = 1.05 \qquad (6)$$

where |b| is the length of the Burgers vector in the α and the β phases. Although the interfaces seem to provide little resistance to the edge segments, any model of slip transmission should account for the residual dislocations generated at the interface.

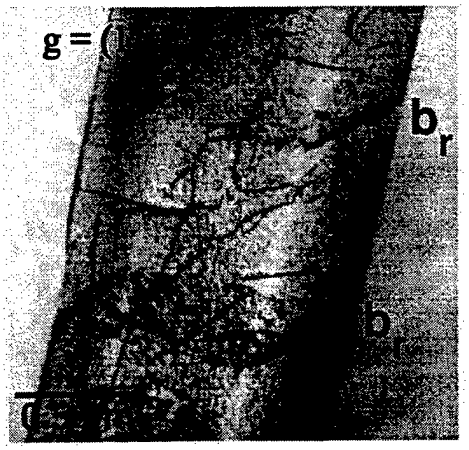

Fig. 19 BF Micrograph showing the contrast from the residual dislocations $\mathbf{b}_r$

In contrast, for the OB crystals tested at the same stress level as OA crystal, edge components were found to be piled-up against the broad face of the β-lath. When the stress level was increased to 95% of the yield strength, shearing of the β-lath was observed along a narrow band and contained dislocations of different Burgers vectors. Near the sheared regions, $\mathbf{a_1}$ dislocation activity in the α phase is also observed. For OB crystal, the slip transmission process has to accomodate not only for the difference in the lengths of the Burgers vectors but also for the misallignment between the slip systems. TEM observations on a foil with its normal parallel to the basal plane (i.e. interaction of the edges with the broad face) suggests that this accomodation is achieved by the formation of non-$\mathbf{b_2}$ dislocations in the β phase and the emission of $\mathbf{a_1}$'s in the α phase.

We propose two simple models to describe the slip transmission in these two oriented colony crystals. Fig. 20 a represents the passage of an $\mathbf{a_1}$ edge dislocation through the β lath, leaving a residual dislocation which equals to $0.05\mathbf{a_1}$ at the entry point. At the exit face of the β lath, another residual dislocation of the same magnitude but of the opposite sign is left behind. A passage of 20 such $\mathbf{a_1}$ edges at the first face will cause the formation of an $\mathbf{a_1}$ dislocation which can now glide on the prism plane into the β phase, Fig. 20 b. At the exit face, the passage of 20 $\mathbf{b_1}$'s will result in the formation of a $-\mathbf{a_1}$ dislocation which glides away from the exit face and annhilates with the incoming $\mathbf{a_1}$, Fig. 20 c. Such an annhilation of the residual dislocation should suggest an inherent low work hardening and poor creep resistance which was experimentally observed.

A similar model for slip transmission on the broad face of an OB sample is shown in Fig. 21. The passage of an $\mathbf{a_2}$ dislocation into a $\mathbf{b_2}$ leaves a residual dislocation which is ~$1/6\mathbf{a_1}$ at the entry face. Similarly at the exit face another residual dislocation of magnitude $1/6\mathbf{b_1}$ is left behind. Again the passage of the 6 dislocations at either face causes the formation of a perfect $\mathbf{a_1}$ dislocation which can then glide away from the interface on its prismatic plane. The formation of these residual dislocations at the interfaceand there inability to annhilate suggests that OB colony crystal should show work hardening and superior creep resistance.

2.4 Compression and Creep Testing for Orientation B

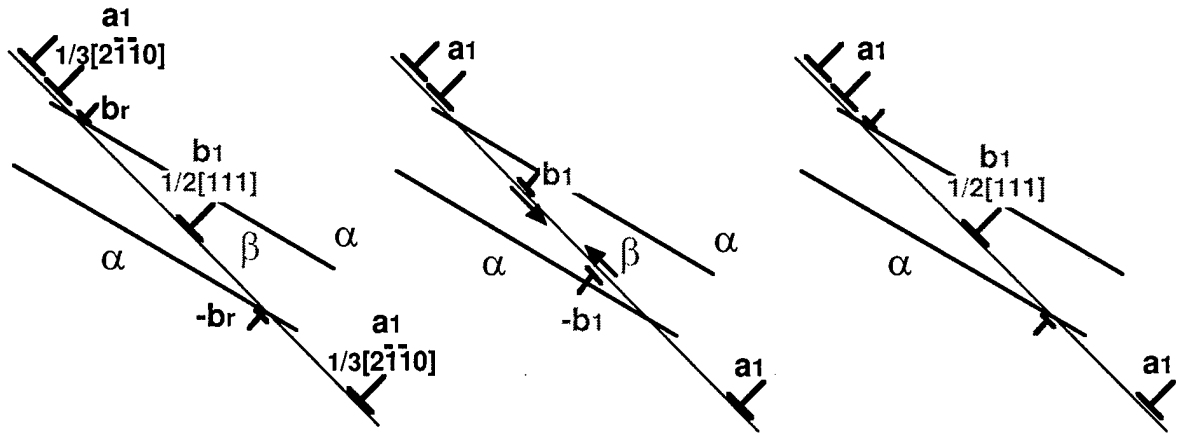

Fig. 20 (a) Passage of an $\mathbf{a}_1$ dislocation leaving behind a $\mathbf{b}_r$ at the interface and the formation of a $-\mathbf{b}_r$ on the exit face, (b) the passage of 20 $\mathbf{a}_1$'s leaves behind an $\mathbf{a}_1$ at the entry face and a $-\mathbf{a}_1$ at the exit face, (c) the two complete $\mathbf{a}_1$'s of the opposite sign glide along the prismatic plane and annhilate one another.

Constant strain rate tests were performed for the two colony crystals, shown in Fig. 22. It is clear that the OA colony crystal shows little strain hardening (n~0) while the OB shows a higher yield strength and more work hardening (n=0.043). The strain rates for the two crystals was similar (m~0.01). For OA crysal, using Equation 1, the value of the time exponent ***a*** should equal 1, i.e steady state flow. Similarly for OB, the value of ***a*** equals 0.19.

In the previous annual report, the experimentally determined time exponent for OA colony crystal was nearly 1. Fig. 23 shows the creep curve on (a) linear-linear and (b) log-log scale for an OB colony crystal stressed at 80% of its yield strength. Two distinct regions are observed - an initial sluggish accumulation of strain which reaches a steady value of 0.2 at longer time. It is also interesting that a comparison of data, shown in Fig. 24 a, b for the different single and two phase poly- and single colony crystals of Ti alloys studied in this program and from data in the literature show this remarkable trend

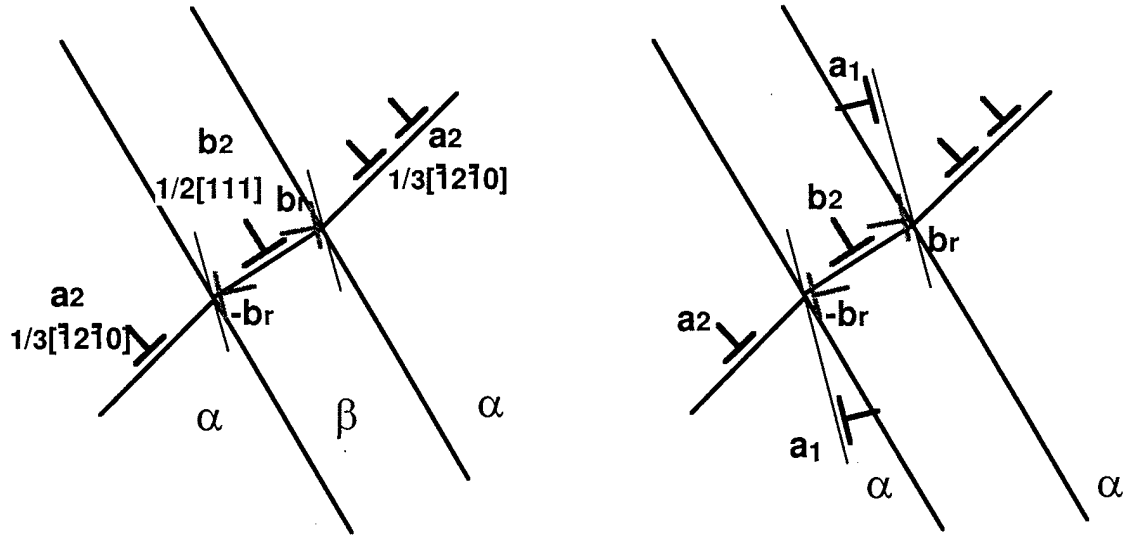

Fig. 21 Schematic showing a possible slip transmission mechanism for OB colony crystal. The inability of the residual dislocations to annhilate suggests more creep resistance.

of reaching a long time exponent **a** of 0.2. Current investigation focusses on determining the dislocation mechanism responsible for the universality of **a** for Ti alloys.

3. In-situ Experiments on single colony crystals

Post-mortem TEM observations have indicated that the shearing of the β laths is a difficult process, as indicated by the observation of pile-ups at the α/β interfaces. At sufficiently high stresses, shearing of the β-laths does occur. We hope to capture and characterize the detailed events associated with the pile-up formation and β-lath shearing processes using these in situ studies.

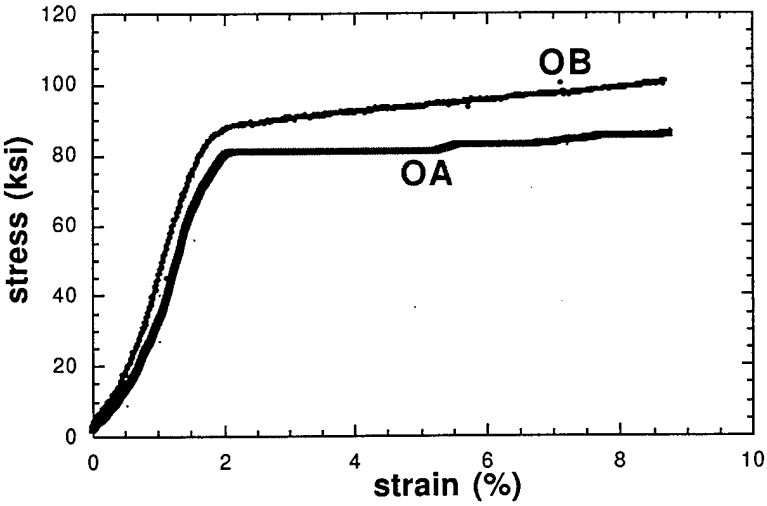

Fig. 22 Constant strain rate tests for oriented single colony crystals for Ti-5Al-2.5 Sn.

The second sample orientation is intended to explore the processes associated with α/β interfacial sliding. This process has been observed at the optical and SEM level, and is recognized as an important deformation mode, even at room temperature. There has been no TEM study of this process however, and *in situ* observations should be particularly revealing of the controlling mechanisms for the sliding

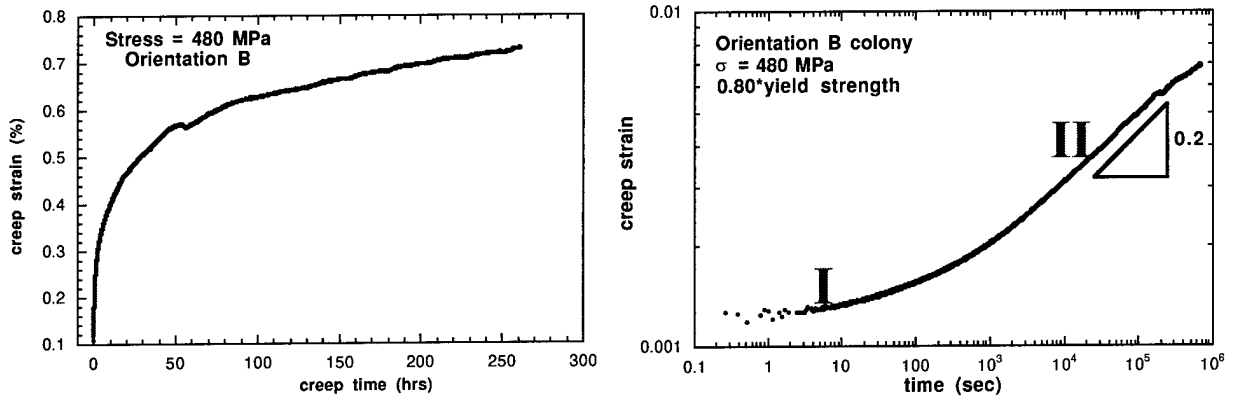

Fig. 23 Creep curve for oriented colony crystal at 80% of its yield strength on (a) linear-linear and (b) log-log plot.

process. One likely mechnism which we have recently proposed is that interfacial dislocations present at the semi-coherent α/β interfaces may respond to applied shear stresses and glide. In particular, a high density of **c**-type dislocations of near-edge character are present on the broad faces of the α/β

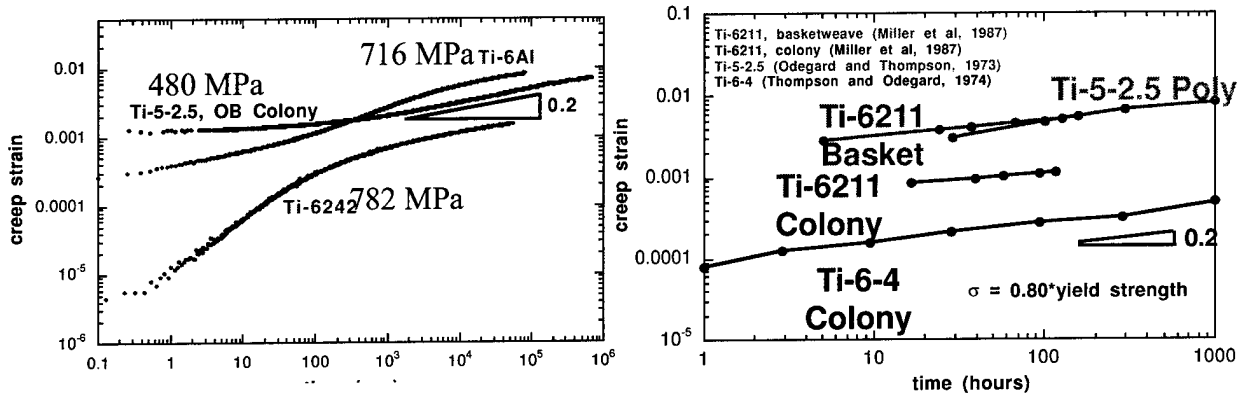

Fig. 24 The time exponent **a** for different single and two phase Ti alloys reaches a constant value of 0.2, (a) experimental results from the present

interfaces. This second sample orientation for the *in situ* studies has been chosen to maximize the shear stress for the motion of these **c**-type dislocations. In situ TEM testing of samples should enable capturing the dynamic aspects of dislocation movement, and their interaction with other structural features on these interfaces. A series of samples for in-situ study were prepared and tested using the Kratos 1.5 MeV microscope at the NCEM in Berkeley, however, we were unable to achieve sufficiently high loads to yield the material. This remains an extremely interesting subject to pursue in this system.

4. Relationship between Primary Creep and Short-Range Ordering

The intense, planar dislocation arrays and slip bands which are prominent in the α-phase of dilute Ti-Al alloys (see Fig. 25a) has long been associated with cutting of short-range-order (SRO) domains. While the presence of SRO has not been directly established in these Ti alloys, long-range ordering and planar, coarse slip has been found in Ti alloys of higher aluminum content [10]. If the relatively low values of n are indeed related to SRO, then it may be possible to significantly reduce the extent of primary creep at lower temperatures by reducing the degree of SRO through appropriate α-field annealing treatments.

A striking indication that this approach may be successful is provided by the results of a recent set of experiments on single-phase Ti-6wt%Al. Two samples have been prepared by annealing high in the α-phase field, at 900°C for 15 minutes in a vacuum evacuated quartz ampule containing Ti getter strips. One sample was then given a slow furnace cool, while the other was quenched in a water bath. The Hollomon parameters obtained from constant strain rate testing of these two samples are shown in Table I. While the yield strengths of the two samples are similar, the rate of strain hardening for the quenched sample is significantly larger, as indicated by the corresponding n values. Assuming that the strain rate sensitivity is unchanged by this treatment (the value of m has not been measured in this preliminary study, but will be in our future work), the value of a predicted based on the Hollomon analysis is about 0.07, compared with a value of 0.25 predicted (and experimentally observed in Figure 1) for the furnace-cooled material. The predicted creep curves for the two conditions are shown in Fig. 26. These results indicate that much more rapid exhaustion should occur in the quenched material,resulting in a significant reduction in primary creep strains.

The reason for the beneficial change in n value has been investigated in a preliminary TEM analysis of deformation microstructures for the two samples shown in Figure 25. Highly planar prism and basal glide is typical of the furnace-cooled sample (Figure 25a), with little dislocation content observed outside of these bands. Deformation localized into such arrays has been noted for alloys exhibiting SRO behavior, such as Ni-Cr alloys [11]. An example of the microstructure in the quenched sample is shown in Fig. 25b. There is a dramatically larger content of dislocations distributed more homogeneously. Contrast analysis demonstrates that most of the homogeneously distributed dislocations are **a**-type, and tilting experiments indicate that the dislocations are lying on both prism and basal planes. Thus, extensive cross-slip appears to have replaced the planar slip mode commonly observed in these alloys. Consider the implications of these observations for work hardening of prismatic slip. In the intense, planar slip mode, the only possibility for hardening involves the intersection of separate dislocation bands. These intersections are relatively infrequent and can easily be overcome by the stress concentrations generated within the bands. Conversely, the high density of basal dislocations in the quenched sample act as numerous forest dislocations to the prism plane activity, leading to latent hardening and higher values of n. In addition, the intrinsic rate of hardening for basal slip is not known, but

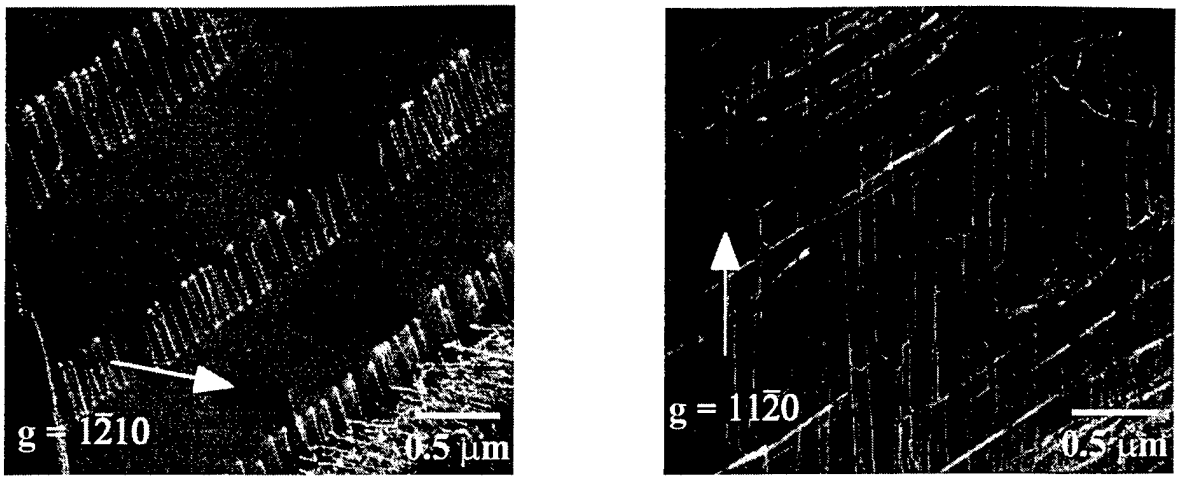

Figure 25 (a) Highly planar and localized slip arrays seen in an α annealed and slow cooled Ti-6wt% Al alloy. (b) Slip is non-planar and homogeneous for an α annealed/ water quenched Ti-6wt% Al alloy.

may be larger than that for prismatic slip. Finally, numerous **c + a** dislocations have also been observed in some grains in the quenched sample, and this slip mode may be more prominent in this condition than in the furnace-cooled state.

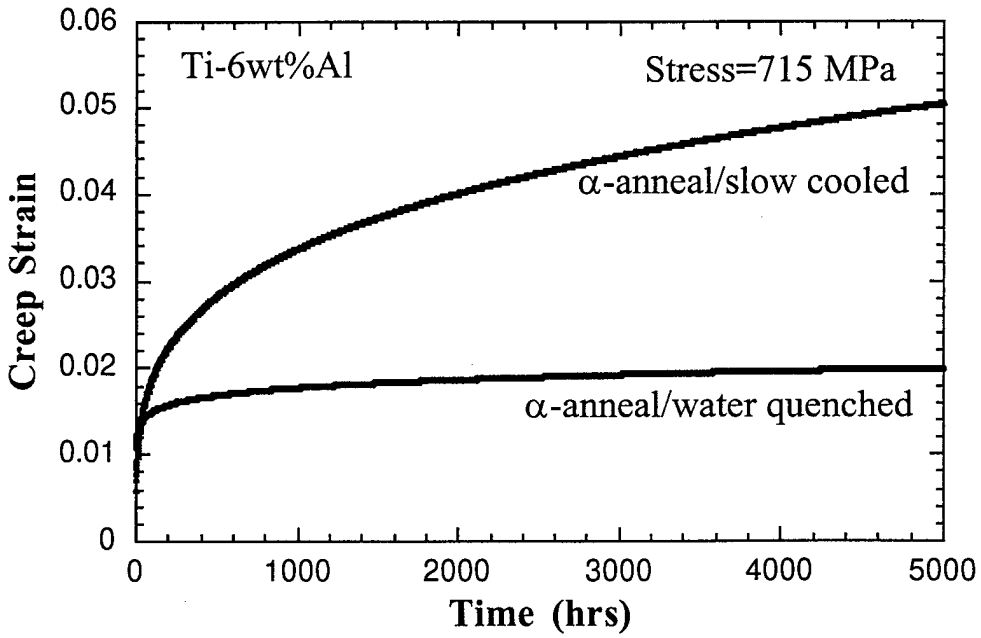

Fig. 26 Predicted creep curves for single phase Ti-6Al alloy for the two heat treaments described in Table II. The water quenched sample has a higher n and a higher creep resistence.

A creep test was performed at a stress level of 716 MPa on a sample subjected to the novel α anneal/ water quench treatment. The creep curve obtained was compared with the creep curve of an α anneal/ slow cooled sample tested at the same stress level. This plot is shown in Fig. 27. It is clear that the form of the creep transient is quite different for the α anneal/water quench sample from that of the α anneal/ slow cooled sample. The α anneal/water quench does not clearly show the three regimes of creep exponent exhibited by the other sample. The long time creep exponent was measured to be 0.11 for the α anneal/water quench sample whereas it was found to be 0.2 for the α anneal/slow cooled samples. But the total strain level for the α anneal/water quench sample was higher than that of the α anneal/ slow cooled sample. Preliminary TEM investigation revealed that as in the case of the α anneal/water quench sample deformed under constant strain conditions this sample also exhibited homogeneous deformation. But there were grains present in the sample which still exhibited planar deformation. Hence, the larger n value exhibited by the α anneal/water quench sample does not seem to have directly translated into higher primary creep resistance. It should be mentioned that this is only a preliminary study and more tests need to be done to confirm this trend.

The fundamental reason for these changes in deformation mode are not presently known. If in fact SRO has been reduced by annealing and quenching, then a reduced tendency for planar slip would be anticipated. It should be noted that the presence of SRO in the dilute Ti-Al alloys is presently only *inferred* from the localized nature of flow.

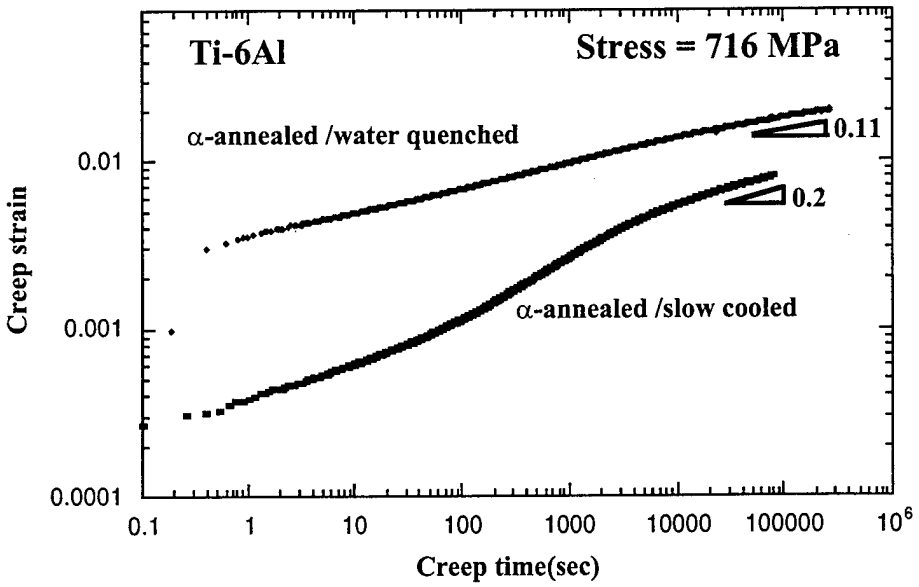

Fig. 27 Comparison of the creep response of the α anneal/ water quench with that of the α anneal/slow cooled at the same stress level(716 MPa).

Recently ageing studies were performed to investigate the possiblity of precipitatingTi_3Al particles in the Ti-6Al alloy. Based on the work of Namboodhiri et al [12] the Ti-6Al sample was aged for 10 hours at 550 ^oC. TEM was done on this sample and diffraction evidence indicating the presence of theTi_3Al was obtained although the precipitates themselves were too small to be imaged. This evidence gives credence to the presence of SRO in the unaged sample causing the heterogeneous deformation.

Difficulties were encountered with the Ti-6Al alloy during the development of heat treatment to decrease the SRO. It was observed that although the sample was single phase at the start, it lead to a two phase structure after being annealed in the beta field and cooled to room temperature. It is possible that the iron content might be high enough to cause the precipitation of the beta phase if the alloy is slow cooled. Improved response should be possible with Ti-6Al of lower iron and oxygen content.

5. References

1. A. J. Hatch, J. M. Partridge and R. G. Broadwell, J. *Mater.*, **2**, 111 (1967).
2. A. W. Thompson and B. C. Odegard, *Metall. Trans.*, **4**, 899 (1973).
3. B. C. Odegard and A. W. Thompson, *Metall. Trans.*, **5**, 1207 (1974).
4. M. A. Imam and C. M. Gilmore, *Metall. Trans A.*, **10A**, 419 (1979).
5. A. K. Chakrabarti and E. S. Nichols, *Titanium '80 Science and Technology*, edited by H. Kimura and O. Izumi, AIME, Warrendale, PA (1981), p. 1081.
6. W. H. Miller, R. T. Chen and E. A. Starke, *Metall. Trans A.*, **18A**, 1451 (1987).
7. L. D. Lubahn and R. P. Felgar, *Plasticity and Creep of Metals*, John Wiley and Sons, New York (1962).
8. A. K. Chakrabarti and E. S. Nichols, *Fourth International Conference of Titanium,* ed. H.Kimura and O. Izumi, Trans. AIME, Kyoto, Japan, p. 1081 (1980).
9. T. Furahara, T. Ogawa., and T. Maki, *Phil. Mag. Letters*, **72**, p.175 (1995).
10. J. C. Williams and M. J. Blackburn, *Phys. Stat. Sol.*, **25**, K1 (1968).
11. N. Clement, D. Caillard and J. L. Martin, *Acta Metall.*, **32**, 961 (1984).
12. T. G. K. Namboodhri, C. J. McMahon and H. Herman, *Met. Trans.*, **4**, 1323 (1973).

PERSONNEL SUPPORTED

Faculty:

Professor Michael J. Mills	Principal Investigator
Professor Glenn S. Daehn	Collaborative Basis (no direct support)

Post Doctoral Associate:

Dr. D.-H. Hou	SEM, TEM and spectroscopic analyses (1996-1997)
Dr. G. Babu Viswanathan	SEM, TEM and spectroscopic analyses (1997-1998)

Graduate Research Associates:

Neeraj Thirumalai	Behavior of single phase alloys/SRO Effects
Satyarth Suri	Behavior of multi-phase alloys

Undergraduate Research Assistants:

Christopher Fountain	Metallography, machining, annealing studies
Jonathan Kline	Metallography, machining, annealing studies

PUBLICATIONS

1. S. Suri, T. Neeraj, D-H. Hou, J. M. Scott and M. J. Mills, "*Effect of α/β Interfaces on Creep Behavior of Single Colony Titanium Alloys at Room Temperature*", Interfacial Engineering for Optomized Properties, Eds. C. L. Briant, C. B. Carter and E. L. Hall, **458** 267-272 (1996)

2. S. Suri, T. Neeraj, G. S. Daehn, D. H.Hou, J. M. Scott, R.W. Hayes and M. J. Mills,"*Mechanisms of Primary Creep in Titanium Alloys at Lower Temperatures*", Creep and Fracture of Engineering Materials and Structure, Eds. J. C. Earthman and F. A. Mohamed, 119-128 (1997)

3. S. Suri, T. Neeraj, G. S. Daehn, D. H.Hou, J. M. Scott, R.W. Hayes and M. J. Mills, "*Mechanisms of Primary Creep in α/β Titanium Alloys at Lower Temperatures*", Mat. Sci. & Eng.A, **234** 996-999 (1997)

M. J. Mills, D. H. Hou, S. Suri and G. B. Viswanathan, "*Orientation Relationship and Structure of a/b Interfaces in Conventional Titanium Alloys*", Boundaries and Interfaces in Materials, Eds. R. C. Pond, W. A. Clark, A. H. King and D. B. Williams, 295-301 (1998)

PRESENTATIONS

"Phenomenological Description of Creep Behavior in α/β Titanium Alloys Using Constant Strain Rate Tests", S. Suri, T. Neeraj, D-H. Hou, G. S. Daehn, M. J. Mills, TMS Fall Meeting, Cincinnati, 1996.

"Microstructural and Mechanistic Study of Primary Creep in Single Phase a Titanium Alloys at Room Temperature", T. Neeraj. S. Suri, D-H. Hou, M.J. Scott, G. S. Daehn, M.J. Mills, TMS Fall Meeting, Cincinnati, 1996.

"Effect of Orientation on Creep Behavior of Single Colony α/β Titanium Alloys at Low Homologous Temperature", S. Suri, D-H. Hou, T. Neeraj, M. J. Scott, G. S. Daehn, M. J. Mills, TMS Fall Meeting, Cincinnati, 1996.

"Effect of α/β Interfaces on Creep Behavior of Single Colony Titanium Alloys at Room Temperature", S. Suri, T. Neeraj, D-H. Hou and M. J. Mills, MRS Fall Meeting, Boston, 1996.

"Mechanisms of Primary Creep in Titanium Alloys at Lower Temperatures", S. Suri, T. Neeraj, G. S. Daehn, D. H.Hou, J. M. Scott, R.W. Hayes and M. J. Mills, International Conference on Creep and Fracture of Engineering Materials and Structures, Irvine, August 1997.

"Mechanisms of Primary Creep in α/β Titanium Alloys at Lower Temperatures", S. Suri, T. Neeraj, G. S. Daehn, D. H.Hou, J. M. Scott, R.W. Hayes and M. J. Mills, International Conference on Strength of Metals and Alloys, Prague, August 1997.

"TEM Investigation of Interfaces in Titanium Alloys (Invited)", M. J. Mills, Joint Meeting of the German, Swiss and Austrian Microscopy Societies, Regensburg, Germany, September 1997.

"Orientation Effects and the Role of α/β Interfaces in Room Temperature Creep Behavior of Titanium Alloys", S. Suri, T. Neeraj, V. Babu, G. S. Daehn, D. H. Hou and M. J. Mills, Symposium on Micro-

structure-Property Relationships in α/β Titanium Alloys, TMS Fall Meeting, Indianapolis, 1997.

"Phenomenological Description of Creep Behavior in α and α/β Titanium Alloys Using Constant Strain Rate Tests, T. Neeraj, S. Suri, V. Babu, G. S. Daehn, D. H. Hou and M. J. Mills, Symposium on Micro-structure-Property Relationships in α/β Titanium Alloys, TMS Fall Meeting, Indianapolis, 1997.

" α/β Interfaces and the Mechanical Properties of Titanium Alloys (Invited)", M. J. Mills, S. Suri, N. Thirumalai and G. B. Viswanathan, D. A. Smith Memorial Symposium, TMS Fall Meeting, Indianapolis, September 1997.

INTERACTIONS / TRANSITIONS

Patent disclosure filed with the Office of Technology Transfer, the Ohio State University on ""Heat Treatement for Short-Range Order Elimination and Improved Mechanical Properties in Ti Alloys". (See Attached Disclosure Statement)

Periodic discussions with Wright Laboratories personnel concerning results obtained and coordination of program with other efforts on titanium alloys at Wright Laboratories.

NEW DISCOVERIES

The minimization or elimination of short-range ordering in the α-phase of titanium alloys is possible through heat treatment and quenching from high in the α-phase field. This modification of SRO results in dramatically different microstructures and offers the potential for improved creep, strain hardening and fatigue properties in Ti alloys at lower temperatures.

"Negative" creep in single phase Ti-6Al has been observed. This highly unusual mechanical response may be related to the unique dislocation arrangement and dynamics in these alloys.

HONORS / AWARDS

• M. J. Mills has been awarded a Von Humbolt Research Fellowship in 1996. The Von Humbolt Research Fellowships are intended to foster interaction between German research institutions and scientists from abroad. M. J. Mills will be visiting the Fredrich-Schiller Institute, University of Jena from June 16-September 12, 1998.

• M. J. Mills has been awarded the American Society for Metals Silver Medal for Research for 1998. This award was established in 1986 to "recognize and honor an active researcher whose

individual and collaborative work has had a major impact on the field of Materials Science. It is intended for someone near mid-career (about 5-15 yrs after final degree), who has personally conducted his or her own research, and who has made a significant contribution." This award will be awarded at the ASM/TMS Fall Meeting in Rosemont, Illinois, October 1998.